WILEY-VCH

Sustainable Additive Manufacturing of Polyelectrolyte Photopolymer Complexes

Thomas J. Kolibaba, Callie I. Higgins, Nathan C. Crawford, Joseph R. Samaniuk, and Jason P. Killgore**

Dr. T.J. Kolibaba, Dr. C.I. Higgins, Dr. J.P. Killgore
Applied Chemicals and Materials Division
National Institute of Standards and Technology
MS 647, Boulder, CO 80305, United States
E-mail: Thomas.Kolibaba@nist.gov
E-mail: Jason.Killgore@nist.gov

Dr. N.C. Crawford
ThermoFisher Scientific
5225 Verona Road, Madison, WI 53711, United States

Prof. J.R. Samaniuk
Department of Chemical and Biological Engineering
Colorado School of Mines
1613 Illinois St, Golden, CO 80401, United States

Keywords: polyethylenimine, vat photopolymerization, stereolithography, digital light processing, recyclability

Polyelectrolyte complexes (PECs), assemblies of oppositely charged polymers with powerful properties and wide-ranging applications, are currently not melt-processable via any conventional means and have been limited commercially to applications only as coatings. Here, a unique strategy of pairing a polycation with an oppositely charged photopolymerizable monomer is employed. Vat photopolymerization of this mixture yields 3-dimensional spatial control over PECs for the first time. The properties of these 3D printed PECs are evaluated and are found to be similar to conventionally studied PEC materials. The water-sensitivity of the PEC parts is adjustable through the incorporation of a small amount of a hydrophilic covalent crosslinker, highlighting potential future applications of these materials in 4D printing. Finally, the upcyclability of the additively manufactured PECs is demonstrated through the dissolution of a printed part and its incorporation into virgin resin to yield a part composed of partially recycled material. This chemistry has the potential to dramatically expand the application space

of PEC materials and is a step towards a more circular economy for the field of additive manufacturing.

1. Introduction

Polyelectrolyte-based materials, commonly comprised of a composite formed by a pairing of two oppositely charged polymers, possess a virtually limitless range of properties that makes them useful in fire protection,[1,2] food packaging,[3,4] drug delivery,[5,6] antifouling,[7] insulation,[8] and more. They are very popular materials because they can be processed in aqueous solvent, are often environmentally benign, and sometimes are bio-based and/or biodegradable.[9–11] While impressive, the application space of polyelectrolyte materials is limited by the challenges presented in their processing. Polyelectrolyte complexes (PECs) are bulk assemblies of oppositely charged polymers, where the sites of interaction between the two species creates a physical crosslink. These physical crosslinks give rise to unique phase behaviors, ultraviscosity, and a response to salinity that mimics the thermoplastic response to temperature.[12–15] Due to the dynamic nature of these ionic bonds, polyelectrolyte complexes possess unique capabilities like recyclability and self-healing that make them very attractive as compared to more conventional polymers.[4,16–19] The unique nature of PEC bonding gives rise to an incompatibility with melt processing, making their processing extremely challenging. As a result, PECs are typically used as coatings where spatial control is only afforded in one dimension (i.e. thickness of the coating) via layer-by-layer assembly.[20–22]

Despite the lack of melt processability, progress in 2D processing of PECs has been achieved by manipulating the flow-ability of the materials via compositional variation. The thermal transition temperatures of PECs (e.g. glass transition T_g) can be tailored by PEC salinity and water content.[23–25] In the last decade, salinity changes have enabled extrusion of PECs.[26] While the advent of extrusion has allowed more facile study of the properties of bulk PECs,[27,28] it has yet to lead to many practical applications outside of compounding PECs into thermoplastics.[29] Despite its early promise as a new means of processing PECs, this form of processing has largely been neglected. Relatedly, the success with extrusion of 2D profiles has not led to adaptation of 3D processing techniques such as injection molding. There is still an outstanding need for the development of 3D processing techniques for PECs to enable more widespread use of these technologies.

Additive manufacturing (AM), also known as 3D printing, has seen increased popularity both industrially and in academics owing to its paradigm-shifting change of the manufacturing process. In particular, vat photopolymerization (VP) has seen significant growth due to its vast manufacturing potential and wide variety of compatible chemistries.[30,31] There are several forms of VP additive manufacturing, but one commonality to all techniques is the formation of solid objects by exposing certain regions of a liquid resin to patterned light. The solidification process is driven by photopolymerizations of mono and/or multifunctional monomers into polymers, causing gelation through the formation of chemical crosslinks. Complex parts are grown layer-by-layer via lifting of a freshly-solidified layer, allowing unreacted resin to flow under the part and be subsequently exposed to a new light pattern.

Photopolymerization has been used to polymerize two-dimensional PECs and PEC coatings, but only polyelectrolyte homopolymers (which have limited practical applications because they irreversibly dissolve in water), not complexes, have been produced via VP.[32–35] There have not yet been any reports of 3D printed PECs by any AM method. Here, a VP-AM technique is demonstrated which yields the ability to generate controlled three-dimensional structures for PECs of photopolymerized poly(methacrylic acid) (PMAA) and the polycation polyethylenimine (PEI) for the first time. Unlike traditional VP resins, this PEI:PMAA resin forms parts on the basis of reversible physical crosslinks instead of permanent covalent ones. This yields photopolymerized parts that can have tunable swelling properties in water (via the incorporation of a covalent crosslinker) and that can be redissolved after pH adjustment and incorporated back into virgin resin to be printed again. The facile upcyclability of the printed PECs puts these materials in very rare company among existing photopolymer resins which typically have little-to-no potential to reuse printed parts. This novel application of polyelectrolyte chemistry offers promise for a more sustainable and circular AM economy in addition to unlocking novel 3D printing chemistries that could enable materials which are intrinsically flame retardant, biocompatible, antifouling, stimuli responsive, or a combination therein.

2. Results and Discussion

2.1. Polyelectrolyte Photocomplexation

The process of photopolymerization of methacrylic acid followed by complexation with PEI is shown in Figure 1. A stoichiometric mixture of neutral methacrylic acid (MAA) and PEI are dissolved in isopropanol along with a photoinitiator (BAPO) to form the photoactive resins. The PEI:MAA:BAPO molar ratio of 105:105:1 (the molar mass of PEI's aziridine repeat unit

was utilized) was held constant across all studied resin formulations regardless of overall concentration. Because of the acid-base reaction between PEI's repeat units and MAA, the monomers are already associated with the oppositely charged polymer in solution prior to polymerization. Other acid species, such as acrylic acid, are known to polymerize faster in their deprotonated state, so this pre-charged system may also increase the reaction rate.[36] Gelation during printing is accomplished by the complexation of the PEI with the photopolymerized PMAA, rather than by covalent crosslinking more typically seen in VP (Figure 1b). A relatively low molecular weight PEI (M_n=600 g mol^{-1}) was used to minimize resin viscosity and maximize solubility. Resins composed of pure PEI:MAA rapidly became too viscous to use in a printer, and the resultant assembly could not be dissolved. The addition of isopropanol (IPA) as a solvent ensures a suitable viscosity for printing. Other stereolithography resins have been developed which make use of ionic coordination via acid-base reactions, but necessitated lower solids content than the PEI:PMAA resin that is used here (66.5 wt% for the highest concentration resin).[37,38] After mixing, the PEI/MAA/IPA resins are shelf-stable so long as they are kept away from light.

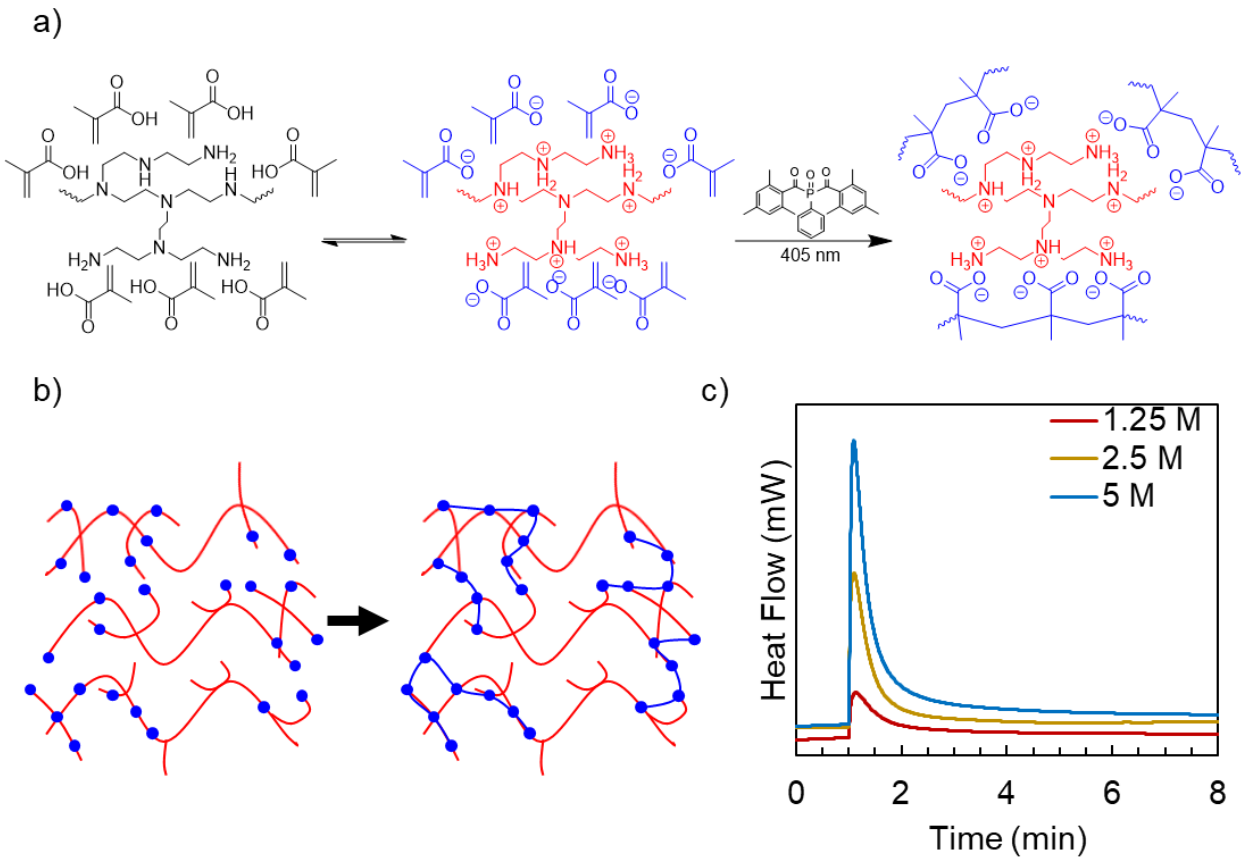

Figure 1. (a) Schematic of the photopolymerization of methacrylic acid yielding a PEI:MAA polyelectrolyte complex. (b) Cartoon depicting the formation of a network between a branched polymer (red, representing PEI) and separate polymer chains (blue, representing PMAA) that form from individual ionic linkages (blue circles) yielding a network that is associated on the basis of ionic interactions and no covalent crosslinking. (c) PhotoDSC plots of the PEC resins.

Differential scanning calorimetry under a UV light source (PhotoDSC) was utilized to study the rate of the polymerization reaction of MAA. This is shown in Figure 1c, with the integrated peaks summarized in Table 1. The width of the peaks in the plot shows that the reactions take slightly longer to complete as the concentration of the resin increases, likely because the viscosity of the solution increases and slows the rate of MAA propagation. The heat evolved from the polymerization (ΔH_{rxn}) measured from PhotoDSC can be used as a proxy for extent of reaction by comparing it to a calculated heat of polymerization (ΔH_{polym}) for a pure material (an example calculation for the 5 M resin is available in the SI).[39] From the tabulated data, it can be seen that heat of reaction is nearly linearly proportional with resin concentration and that extent of reaction is consistently just above 50 %. Deviations from linearity in this system could be explained by a more rapid evaporation of solvent out of the resin in the more exothermic systems providing a lower apparent enthalpy. Measured conversions of <60 % in

PhotoDSC are relatively low as compared to most photopolymer resins.[35,39–41] However, the effective functionality of ionically associated PEI:MAA will be extremely high. The number average degree of polymerization of PEI is around 14, and it can be safely assumed that many of those repeat units at any given instant are coordinated with a methacrylate anion. High levels of functionality lower the conversion required to achieve gelation, and as a result parts are able to be printed even with this apparently lower conversion percentage.[42–44]

Table 1. PhotoDSC data for 1.25, 2.5, and 5 M resins.

Resin	ΔH_{rxn} [J/g]	Time to peak [s]	[MAA] [wt %]	Extent of reaction[a)] [%]
1.25 M	47 ± 3	8.7 ± 0.5	10.8	56 ± 4
2.5 M	90 ± 4	6 ± 1	21.5	54 ± 2
5 M	175 ± 2	6.4 ± 0.5	43.0	52.7 ± 0.6

a) Enthalpy of reaction for methacrylic acid was taken to be 771 J g^{-1}, based upon its radical propagation rate constant.[45]

To assess the ability of the PEC resins to print via layered VP-AM, working curve measurements were performed. Working curves measure the depth of a cured layer versus light exposure dose to determine critical exposure dose for gelation and depth of light penetration.[46] The working curves for the PEC resins were determined by exposing PEC resin to light doses (from a ca. 2.3 mW cm^{-2} light source) ranging from 4.6 mJ cm^{-2} to 74 mJ cm^{-2} with a 1 mm x 1 mm illumination pattern and measuring the heights of the resultant pillars (Figure 2). To ensure substrate adhesion for the measurement, the pillars were polymerized on methacrylate-functionalized glass slides.[47] The dramatically different critical dose for gelation highlights the importance of polyelectrolyte concentration on its ability to photocomplex. The 2.5 M resin requires a more than 3-fold light dose (by comparing E_c, the critical light dose) as compared to the 5 M resin just to reach the gel point. The working curve measurement differs from the actual printing process in that there is no vertical confinement from a build plate (since it is cured to a glass cover slip) and the cured material does not need to survive the stress of the build plate lift step. Thus, printing parameters cannot be directly extracted from the working curve. For example, delivering a light dose corresponding to a 100 μm cure depth (a roughly 2 s exposure on the printer studied) on the working curve does not yield enough solid to adhere to the build plate. Instead, 5.25 s layer times (≈12 mJ cm^{-2}) were utilized, which the working curve would predict to generate a layer thickness of ≈365 μm, to print 100 μm layers with the 5 M PEC. This disparity may be a result of the lack of oxygen inhibition (i.e. the termination of growing chains

by oxygen dissolved in the resin) at the substrate-resin interface when making the working curve on glass as opposed to the fluorinated ethylene propylene film in the LCD printer. The need to polymerize past the cure depth could also be a consequence of needing enough interlayer strength for the material to adhere to the build plate or the previously polymerized layer.[48,49]

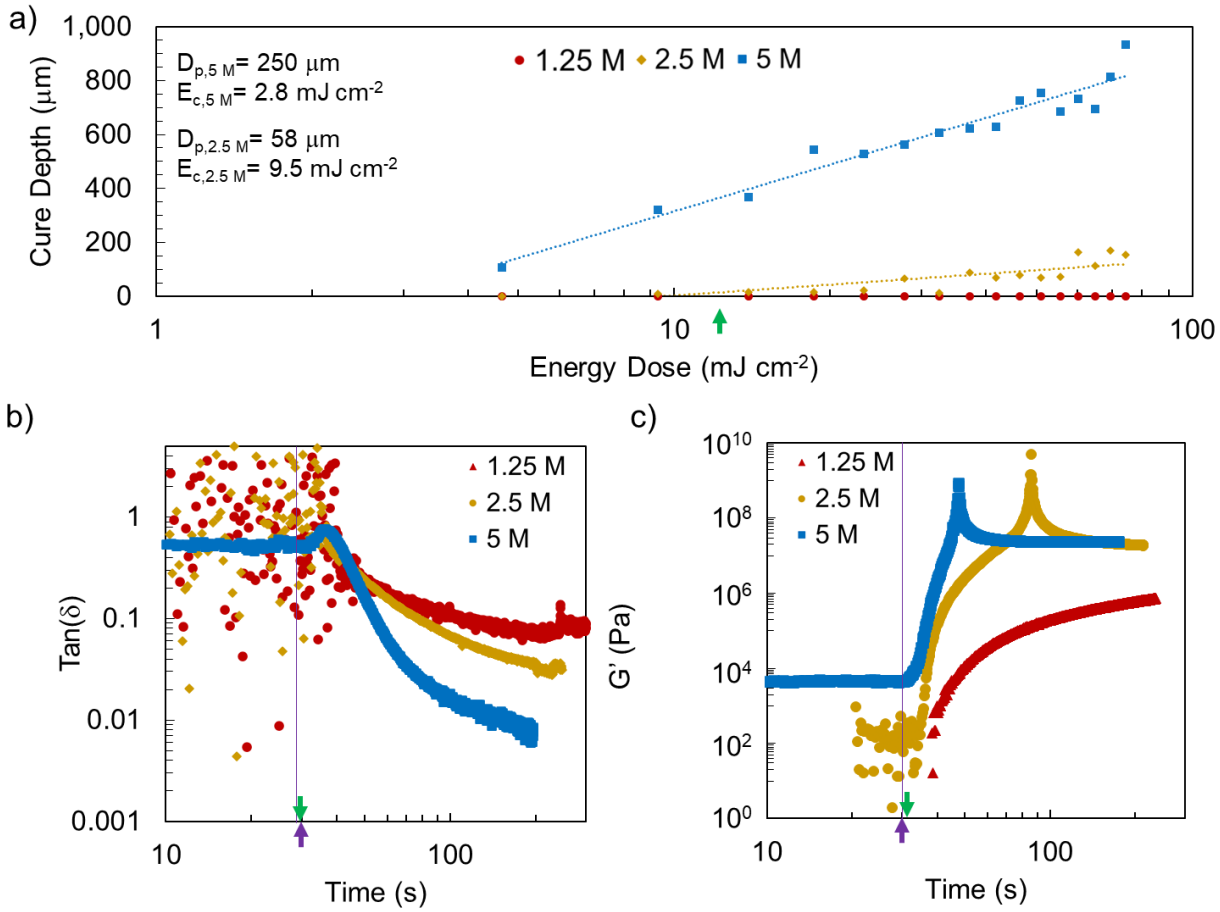

Figure 2. (a) Working curves for three concentrations of PEI:MAA resin along with fit parameters of depth of light penetration depth (D_p) and critical dose (E_c). (b) Plot of tan(δ) vs time for PEI:MAA resins in photorheology. The purple line indicates the onset of UV exposure (30 s after data acquisition begins). The green arrows in each panel indicate the dose used for printing. (c) Plot of storage modulus vs time for PEI:MAA resins in photorheology.

The three studied resins exhibit significantly different working curves, with the 2.5 M resin exhibiting a much shallower response in cure depth to the delivered light dose than the 5 M resin. The 1.25 M resin did not form any solid at all. According to the curve fit equations, it would take nearly 500x longer per layer to print the 2.5 M PEC (assuming a cure depth of 365 µm from the working curve universally correlates to a successful 100 µm layer). Typically, photopolymer additive manufacturing processes set layer times as close as possible to the minimum network formation time to improve printing throughput and avoid lateral over-

polymerization. It has been shown recently that, in thermally initiated polymerizations of an anionic monomer in the presence of a polycation, the size of the PEC aggregates formed scales dramatically with concentration of the polyelectrolyte.[50] Similar aggregates may form prior to the formation and precipitation of a PEC network in this printing process. As a result, maximizing solids (i.e. nonsolvent) content of a VP resin is critical to print success.

Photorheology can be used to understand the kinetics of photocuring and the gel point of a given resin. The gel point is of particular interest in VP printing, because this point can indicate when a layer is solid enough to continue the printing process. The gel point is typically defined as the crossover in the storage and loss moduli of a material (i.e. when the loss tangent, which is the ratio of loss modulus to storage modulus, drops below 1) and the material transitions from a liquid-like solution to an elastically dominated gel-like semisolid.[51,52] Interestingly, as shown in Figure 2b, the 5 M resin begins with a loss tangent <1 from the onset of study, while the lower concentration resins are of sufficiently low viscosity to approach the lower limit of torque sensitivity of the rheometer prior to the beginning of irradiation. The initial tan(δ) values less than 1 prior to polymerization that were observed for the 5 M resin may be due to very high intermolecular forces between the salted PEI:MAA units, leading to more elasticity at the 10 Hz frequency used for the photorheology experiments. The "spike" in tan(δ) for the 5 M resin shortly after the onset of irradiation is uncommon in most photopolymer resins. The brief increase in tan(δ) before it begins to decline indicates a rearrangement of the forces that cause the 5 M resin's initial elasticity. The early phases of polymerization may create localized heat that decreases the viscosity of the medium before the ionically bound network begins to form. A similar "spike" is also observed in the plot of storage modulus but occurs farther after the initiation of polymerization than the peak in tan(δ) (Figure 2c). The peak appears several seconds after the onset of UV irradiation, as the storage modulus nears its apparent plateau. This could be a result of the ultraviscosity of PECs (where viscosity ~ M_w^5) dramatically increasing the modulus of the material as the initial network forms before slippage across the ionic bonds leads to relaxation and a plateau in the shear modulus.[13] Only the two resins which formed solid in the working curve experiment exhibited this spike in G', further suggesting a critical concentration required to form a network. The plot of tan(δ) versus time also demonstrates the difference in curing kinetics between the three resins, as the loss tangent of the 5 M resin falls significantly faster than the other two.

2.2. Additive Manufacturing of Polyelectrolyte Complexes

Photographs of parts printed from the 5 M resin can be seen in **Figure 3a**. The boat structure demonstrates some important properties of this printing system. First, it can be used to print overhanging features, such as the steering wheel, along with more robust overhanging structures like the roof. Additionally, the PEC parts very closely match the programmed dimensions for printing. Cylinders printed for mechanical property and swelling measurements exhibit a volume shrinkage <5 % compared to the programmed dimensions. A long-hypothesized issue with the additive manufacturing of solid PECs was their dimensional instability when exposed to the aqueous salt solutions required to process them.[26,27] Unlike conventional PEC processing, the studied resins here are prepared in isopropanol. Organic solvents have been shown to have a desiccating effect on PECs, and do not swell dry PECs appreciably.[53] To further understand the interaction of water with additively manufactured PEC parts, printed items were subjected to thermal curing conditions. In other polyelectrolyte systems with similar chemistries this form of thermal treatment leads to the formation of amide and/or anhydride bonds between the PEI and PMAA.[8,54,55] The introduction of covalent crosslinking to these systems is hypothesized to provide improved part durability and increased stiffness.

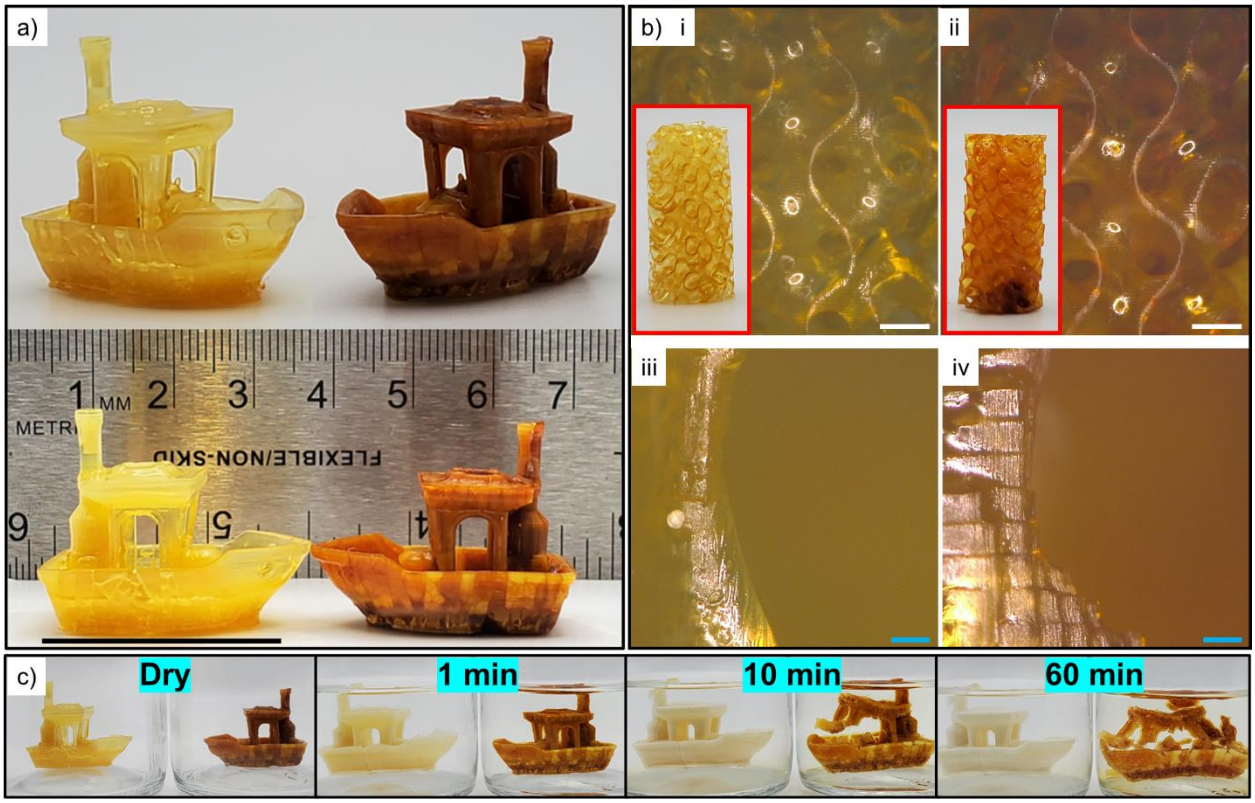

Figure 3. (a) Photos of the as-printed 5 M PEC boats on the left and thermally crosslinked boats on the right. (b) Optical microscope images of a gyroid lattice printed from the 5 M PEC without thermal curing (i, iii) and after thermal curing (ii, iv). Insets show photographs of full cylindrical lattices, programmed diameter =13 mm, programmed height =25 mm. White scale bars represent 1 mm, blue scale bars represent 100 μm. (c) Time lapse photographs of the as-printed and thermally crosslinked boats exposed to water.

The thermal-crosslinking has a clear effect on both the color and optical clarity of the printed parts, as evidenced by the appearance of the crosslinked boats in Figure 3a. Microscope images comparing the as-printed and thermally-cured PEC parts are shown in Figure 3b. It's clear from these images that the elimination of water from the thermal-crosslinking process does not visibly alter the dimensions of the part. However, the individual printed layers stand out more sharply in the thermal-crosslinked part. It is likely that these lines are "smoothed out" by the as-printed PEC's higher hydrophilicity as the part absorbs a small amount of moisture from the air. A comparison of as-printed and thermally-cured PECs when exposed to water is shown in Figure 3c. While the macroscopic swelling of the thermally cured system is lower than in the as-printed system, the part quickly fails and breaks into several pieces. This swelling and failing phenomenon is not observed in extruded traditional PECs.[26] Since the amine groups of PEI are coordinated to MAA through an acid-base interaction prior to printing, it is possible that this creates a more segmented network that could cause fragility of this system when exposed to water. This failure may also be a consequence of the lower molar mass of PEI that

was used (M_n = 600 g mol^{-1}) because of the unprintable viscosity arising from a more commonly used molar mass of PEI (>10,000 g mol^{-1}). A lower molar mass would yield fewer ionic crosslinks to hold the printed object together and a less interconnected network.

In order to attain a more cohesive network, a small amount (1 wt%) of poly(ethylene glycol) diacrylate (PEGDA) was added into the 5 M PEC resin. The incorporation of PEGDA provides a small amount of covalent crosslinking to the PMAA and was hypothesized to be capable of providing a more coherent networked structure capable of excluding water once thermally cured. The PEGDA-PEC did not alter the print parameters from the native 5 M PEC resin, which can be seen by comparing the working curves of the 5 M resin with and without PEGDA (**Figure S1**). When printed with the established parameters for the 5 M PEI:MAA resin, the PEGDA-PEC resin yielded parts with good surface finish, which can be seen in **Figure 4a**. The parts appear more transparent than the parts printed from the 5 M PEC resin. This may be due to the PEGDA improving the interfaces between PEC domains leading to less light scattering.

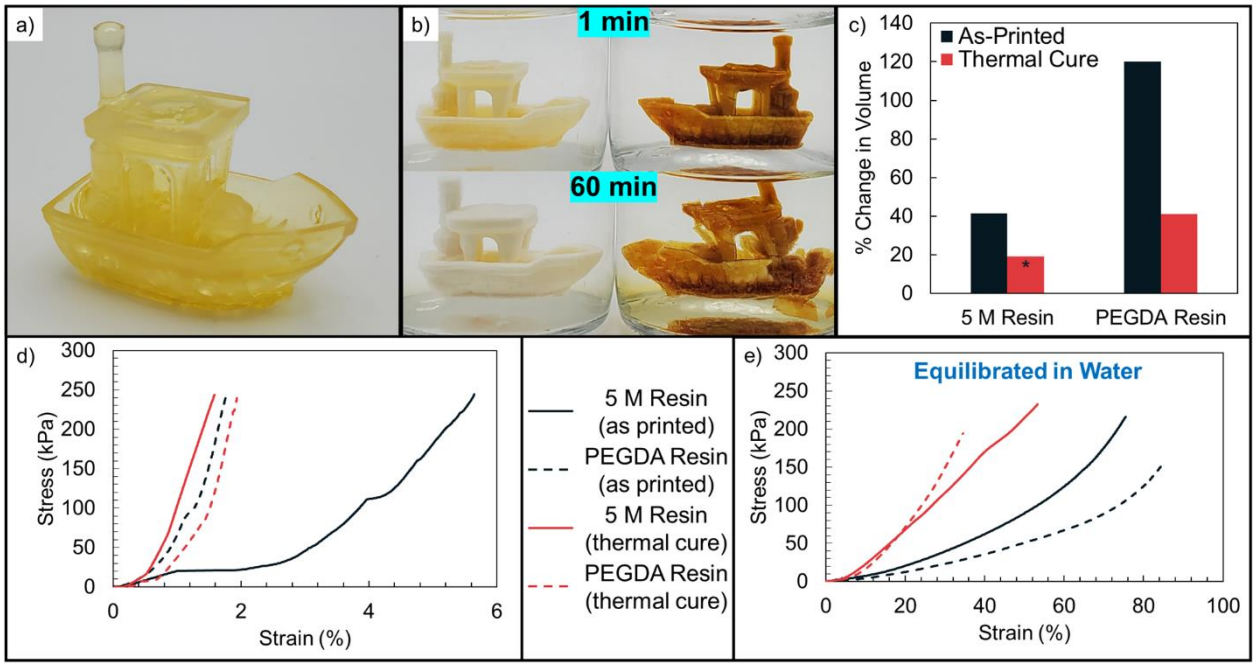

Figure 4. (a) Photos of the as-printed PEGDA-PEC boat. (b) Time lapse photographs of as-printed (left) and thermally-cured (right) PEGDA-PEC parts. (c) Increase in volume of printed cylindrical compression test specimens when exposed to water as a function of PEGDA content and thermal cure. Asterisk denotes a measurement based off a single specimen. (d) Compresive stress-strain curve of dry 5 M PEC and PEGDA-PEC parts. (e) Compressive stress-strain curve of hydrated 5 M PEC and PEGDA parts.

The addition of PEGDA did not serve to significantly improve the durability of thermally cured parts in water, as shown in Figure 4b. The addition of the covalent crosslinking

in addition to the ionic crosslinking caused the resin to be significantly more sensitive to water. Parts printed for compression testing from the PEGDA-PEC resin swelled to over double their volume after exposure to DI water overnight (Figure 4c) while the compression specimen printed from the 5 M resin swelled by only ≈40 %. The extreme increase in water uptake is likely a result of PEGDA's highly hydrophilic nature.[56] For both the 5 M resin and the PEGDA-PEC resin, the thermal cure reduces the susceptibility of the parts to swelling. However, without the presence of PEGDA the thermally cured compression samples consistently failed during water immersion, with only a single sample surviving the water exposure for dimensional measurement and compression testing.

Representative compressive stress-strain curves are shown in Figure 4d and 4e, with tabulated modulus values in Table S1. In all cases except for the dry PEGDA-PEC resin, the parts become stiffer after thermal curing. It is notable that there is considerable deformation of the dry 5 M resin parts in the early phases of compression testing. This is likely due to the presence of collapsible voids in the structure due to the presence of solvent in the resin. A thermal cure or the presence of PEGDA makes these pores strong enough to resist collapse during compression testing. Pores could be avoided in future iterations of this resin by incorporating a reactive diluent.[57,58] The stress-strain curve in Figure 4e highlights once again the extreme sensitivity of the PEGDA-PEC parts to the presence of water, with a compression of >80 % possible without failure. The biocompatibility of many PECs and this adjustable dimensional change in aqueous environments gives additively manufactured PECs potential uses in regenerative medicine as this photopolymerization technique becomes better understood in the future.[59] Further studies could also reveal means of programming differential dimensional change into the printing process and yield 4D printing of these materials.[60]

2.3. Upcycling and Reprinting of Polyelectrolyte Complexes

Polyelectrolyte complexes are well known for their dynamic bonds, which can be influenced by hydration and salt to affect their mechanical properties and phase behavior.[12,15,27] The reversibility of their ionic interactions has led to functional PEC hydrogels and coatings being used as self-healing materials.[16,61,62] Owing to the lack of conventional covalent crosslinkers, additively manufactured polyelectrolyte homopolymers have been shown to be water soluble.[35] As shown in Figures 3 and 4, printed PEC parts are not soluble in water due to the ionic linkages between the chains. **Figure 5** shows that a printed PEC (without PEGDA) part can be dissolved in a basic solution to reverse its ionic crosslinks. Exposure to a 1 M NaOH solution overnight yields a homogenous solution. This is done by deprotonating the

PEI groups, yielding a mixture with highly charged PMAA and little-to-no charge on the PEI molecules. The printed PEC was found to be soluble while accounting for as much as 15 wt% in 1 M NaOH.

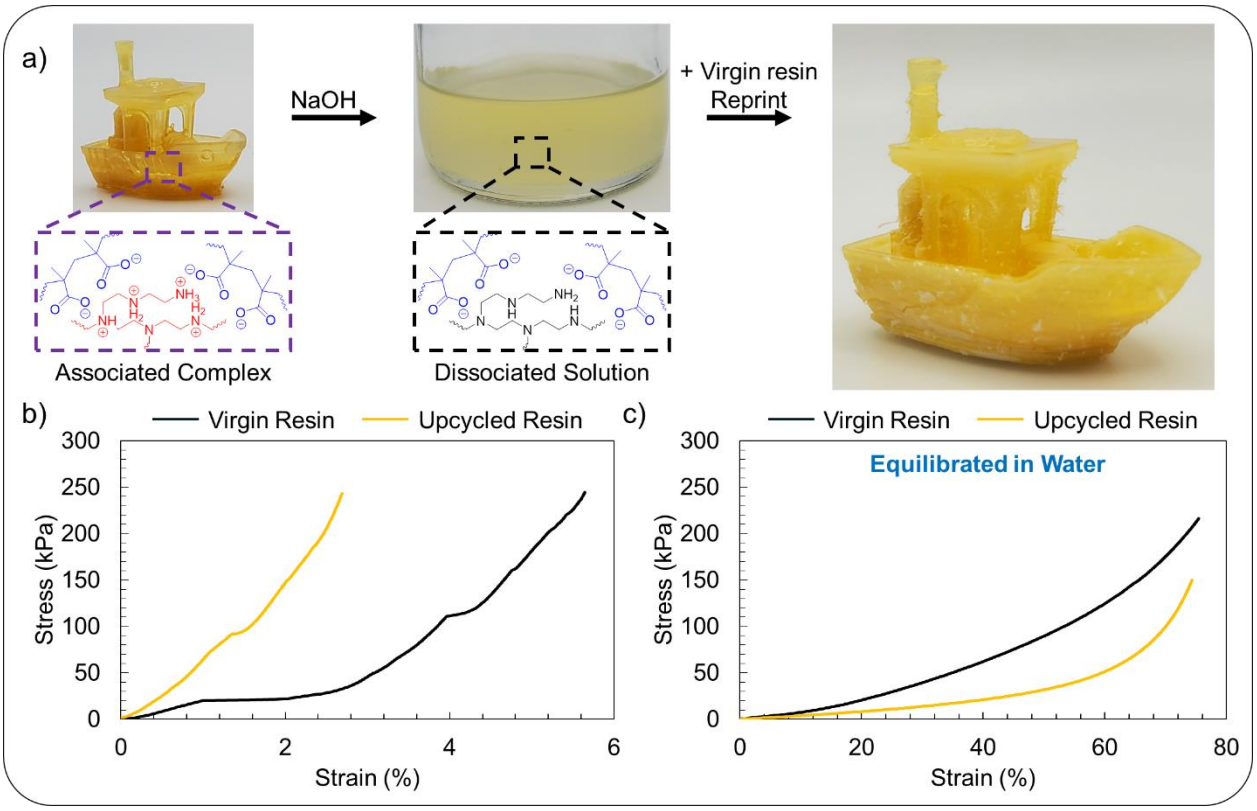

Figure 5. (a) Upcycling and reprinting of an additively manufactured polyelectrolyte complex. First, a printed PEC part (first photograph) is dissolved in base (second photograph), which is then incorporated into virgin resin and reprinted into a new part (final photograph). Schematic illustrations of the chemical transformations throughout this process are shown in the insets. (b) Ambient condition compressive stress-strain plot comparing a representative upcycled PEC and the as-printed 5 M PEC from virgin resin. (c) Compressive stress-strain plots of samples after equilibration in DI water.

After the printed part is fully dissolved, the part solution can be reincorporated into virgin resin as a 5 wt% additive. Due to the presence of acidic protons from methacrylic acid in the virgin resin, some of the PEC precipitates in the mixed resin solution. However, it is very loosely complexed due to the high PEI:PMAA ratio leading to a low driving force for complexation. The resultant slurry can be stirred to homogeneity by hand and poured into the printer vat for reprinting. Upcycled parts are printed under the same conditions as the virgin resin and are shown in the farthest right panel of Figure 5a. It is clear from the photos that the surface finish is poorer, likely a result of light scattering from the presence of precipitated PEC. This issue could be corrected with existing software approaches that account for the scattering

of a resin during the printing process.[63] A compressive stress-strain plot of the upcycled PECs compared to the virgin PECs are shown in Figure 5b-c, with modulus values summarized in Table S1. The presence of dissolved and reincorporated PEC improves the modulus of the studied specimen, especially at lower stresses where early deformation was apparent in the virgin PEC. It is possible that in the dry case, the upcycled PEC acts as an ionically bound filler to reinforce the structure. The hydrophilic nature of the filler may lead to exaggerated softening when the material is hydrated and thus the decreased modulus observed in Figure 5c. The ability to upcycle and reprint parts represents a step towards a more circular economy for photopolymer additive manufacturing. Presently, photopolymer resins yield highly covalently crosslinked materials which are challenging or impossible to break down over time.[64] While the recycled content is somewhat low, the simplicity of the dissolution process (as compared to the energy and time intensive grinding that would be required of other photopolymer resins) offers promise for facile upcycling of these materials.[65] Future work will endeavor to increase the reused fraction of these parts to enable a true chemical recycling process. The unique phase behavior of polyelectrolyte complexes offers a new avenue towards a more responsible use of resources in the additive manufacturing field.

3. Conclusion

Historically, polyelectrolyte complexes have only been able to be processed as coatings that effectively have one dimension of control (i.e. thickness). In this work, a polyelectrolyte complex was additively manufactured for the first time via vat photopolymerization. The printed parts are durable, and through a combination of hydration, thermal curing, and added crosslinker, have tunable dimensions and mechanical properties. Additionally, the reversible nature of the ionic bonds of polyelectrolyte complexes makes these materials uniquely suited to upcycling and reprinting, which is rare in photopolymer materials. The ability to upcycle these materials represents an important step towards a circular economy for the field of photopolymer additive manufacturing. Most importantly, this work enables future studies into the synthesis of three-dimensionally patterned polyelectrolyte complexes with the potential to yield additively manufactured parts with high biocompatibility, biodegradability, and fire resistance. The demonstrated responsivity to both water and pH indicates that these materials also hold promise in the emerging field of 4D printing.

4. Experimental Section

4.1 Materials and Resin Formulation

Branched polyethylenimine (PEI, M_n = 600 g mol^{-1}, M_w = 800 g mol^{-1}), phenylbis(2,4,6-trimethylbenzoyl)phosphine oxide (BAPO, 97 %), poly(ethylene glycol) diacrylate (PEGDA, M_n = 575 g mol^{-1}), acetic acid (glacial, ReagentPlus ≥99 %), 3-(trimethoxysilyl)propyl methacrylate (98 %), and sodium hydroxide (NaOH, BioXtra ≥98 %) were purchased from Sigma-Aldrich (St. Louis, MO, USA). Methacrylic acid (MAA, 99 %, stabilized with 100 ppm to 250 ppm hydroquinone or 4-methoxyphenol) was purchased from Fisher Scientific (Pittsburgh, PA, USA). Isopropyl alcohol (IPA, technical grade) was purchased from Rocky Mountain Reagents (Golden, CO, USA). All water used was deionized.

Additive manufacturing resins were nominally 5 M with respect to both MAA and PEI's repeat unit (aziridine), with a ≈105:1 MAA:BAPO molar ratio dissolved in IPA. For reference, a 5 M resin would contain 21.5 wt% PEI, 43.0 wt% MAA, and 2.0 wt% BAPO (with the balance being IPA). Resins were prepared by first dissolving MAA and BAPO in IPA. This mixture was then chilled in an ice bath while stirring. PEI was then added dropwise to mitigate the heat of solvation and the acid-base reaction that occurs between MAA and PEI. The 2.5 M resin and 1.25 M resin were prepared with 50% or 25%, respectively, of the solids used in the 5 M resin. For resins containing the covalent crosslinker PEGDA, 1 wt% of PEGDA was added in place of IPA after complete dissolution of the PEI (e.g., in 100 g of resin, 1 g of PEGDA would replace 1 g of IPA).

Parts were upcycled by preparing a solution of 15 wt% printed part in 1 M NaOH. This solution was heated in a 70 °C oven overnight, and the cooled solution was added to a batch of virgin resin at 5 wt% loading.

4.2 Part Fabrication

All parts were printed on a Photon M3 405 nm LCD printer (Anycubic, Shenzen, China) that was measured to have an optical power output of 2.3 mW cm^{-2} (PM100D, Thorlabs, Newton, NJ, USA). CAD models of test specimens were sliced to 100 μm layers and exported as a print file in Photon Workshop (Anycubic, Shenzen, China). Prints were carried out with 4 initial "burn-in" layers with 75 s of irradiation to improve adhesion to the build plate, and all subsequent layers were printed with a 5.25 s irradiation time per layer. Between layers the build plate was lifted 6 mm at 0.5 mm s^{-1} and retracted (i.e. lowered into vat to sepecified layer thickness) at 3 mm s^{-1}. All parts were allowed to rest in ambient conditions (21 °C, 50 % relative humidity, and 101.4 kPa atmospheric pressure) for at least 3 days before characterization.

Parts for compression testing and cylindrical lattices were designed in nTopology (nTopology, Inc. New York, NY, USA). Compression samples were designed as solid cylinders with a 10 mm diameter and 5 mm height. Latticed cylinders were created by using the 'Walled TPMS' function in nTopology on a 13 mm diameter, 25 mm tall cylinder. The gyroid cell size was set to (5x5x5) mm^3 with a 0.25 mm wall thickness. Ben the Floating Benchmark (aka Benchy) was downloaded from Thingiverse. Swelling demonstrations were performed by soaking printed parts in deionized (DI) water overnight. Thermally cured parts were placed in a 100 °C oven for 8 hours, and the temperature was then changed to 120 °C for 96 hours prior to testing.

4.3 Characterization

PhotoDSC and photorheology experiments were performed on a Q200 DSC (TA Instruments, New Castle, DE, USA) and on a HAAKE MARS 60 rheometer (ThermoFisher Scientific, Karlsruhe, Germany), respectively. Each instrument was connected to an Omnicure S2000 (Excelitas Technologies, Waltham, MA, USA) broad spectrum UV curing system that was coupled fiber-optically to the instrument. The light was filtered with a 400-500 nm bandpass filter to more closely mimic the printing wavelength of 405 nm.

Samples for PhotoDSC were prepared by placing 2 mg to 3 mg of resin into the bottom of an aluminum Tzero pan (TA Instruments, New Castle, DE, USA). Due to the volatility of IPA, pieces of a glass coverslip (ca. 200 μm thick) were placed over the sample and reference pans to minimize evaporation. PhotoDSC experiments began by equilibrating the samples with a 60 s isothermal step held at 25 °C. After this equilibration step, the light shutter was opened and the samples were allowed to photocure for 10 minutes before the shutter was closed. The light was run at its lowest intensity setting of 3.5 mW cm^{-2} (reported by the instrument).

Samples for photorheology were prepared by pipetting resin (≈1 mL) onto the bottom stainless-steel rheometer plate. The loaded sample was then dispersed between the bottom plate and upper measuring geometry, which consisted of a 20 mm diameter exchangeable quartz glass plate and steel shaft with integrated mirror. Due to significant differences in solution viscosity, the gap between the quartz upper geometry and the bottom plate was varied between 1.2 mm (5 M) and 0.3 mm (1.25 M). The UV light source, which was mounted to the rhomeeter measuring head, was passed through a collimator and directed vertically downward through the upper glass plate via the integrated mirror. All samples were analyzed via time sweep using small-amplitude oscillatory shear with a constant strain value of 0.05% at a frequency of 10 Hz to ensure a sufficient number of data points. Samples equilibrated at 25 °C for 30 s before light

exposure began. Light exposure was constant at 9.48 mW cm^{-2} (measured by a power meter) until the experiment was terminated.

A working curve for each resin was generated by inputting a .stl file of 16 square columns that were 1x1 mm^2 in size. This file (**Figure S2**) was sliced into 16 layers (each with one fewer square than the last) to create 16 exposure conditions. Resin was placed directly on a methacrylate functionalized[47] glass cover slip (No. 1 Corning cover glass, purchased from Sigma Aldrich) on the printer LCD screen and the .stl file was "printed" with no build plate. Excess resin was poured off and the slides were allowed to sit at ambient conditions for 2 hours. Height of the 16 regions was measured with a VL-50A Litematic low force measurement system (Mitutoyo America, Aurora, IL, USA) to produce the measured cure depths for the working curve.

Mechanical properties were measured on a Q800 DMA (TA Instruments, New Castle, DE, USA). Cylinders (ca. 10 mm diameter and 5 mm tall) were placed in the compression clamp and a stress/strain curve was generated by measuring displacement as applied force was increased from 0 to 18 N (loading rate = 1 N min^{-1}). Compressive moduli were calculated from either the first 2 N of force (low-stress modulus) or the final 2 N of force (high-stress modulus). Hydrated parts for mechanical property testing were soaked in DI water for 16 hours prior to testing and were placed in the DMA immediately after removal from water. Optical microscopy was performed on a VHX 600 microscope (Keyence, Osaka, Japan).

Supporting Information

Supporting Information is available from the Wiley Online Library or from the author.

Acknowledgements

This work was performed while Thomas Kolibaba held a National Research Council Associateship Award at the National Institute of Standards and Technology (NIST). Certain commercial equipment, instruments, or materials are identified in this paper to specify the experimental procedure adequately. Such identification is not intended to imply recommendation or endorsement by NIST. Contribution of NIST, an agency of the U.S. government; not subject to copyright.

The authors acknowledge Prof. Alan Sellinger and Caleb J. Chandler (Colorado School of Mines) for assistance with PhotoDSC measurements as well as Dr. Benjamin W. Caplins (NIST) for helpful discussions.

Received: ((will be filled in by the editorial staff))

Revised: ((will be filled in by the editorial staff))

Published online: ((will be filled in by the editorial staff))

References

[1] X. Cheng, L. Shi, Z. Fan, Y. Yu, R. Liu, *Polym. Degrad. Stab.* **2022**, *199*, 109898.
[2] N. A. Vest, T. J. Kolibaba, A. O. Afonso, S. A. Kulatilaka, E. T. Iverson, J. C. Grunlan, *ACS Appl. Polym. Mater.* **2022**, *4*, 1983.
[3] H.-C. Chiang, B. Eberle, D. Carlton, T. J. Kolibaba, J. C. Grunlan, *ACS Food Sci. Technol.* **2021**, *1*, 495.
[4] J. Li, G. van Ewijk, D. J. van Dijken, J. van der Gucht, W. M. de Vos, *ACS Appl. Mater. Interfaces* **2021**, *13*, 21844.
[5] J. J. Chou, A. G. Berger, S. Jalili-Firoozinezhad, P. T. Hammond, *Acta Biomater.* **2021**, *135*, 331.
[6] L. Ge, X. Tan, R. Sheng, J. Xiao, *Colloid Interface Sci. Commun.* **2022**, *47*, 100603.
[7] T. Gnanasampanthan, C. D. Beyer, W. Yu, J. F. Karthäuser, R. Wanka, S. Spöllmann, H.-W. Becker, N. Aldred, A. S. Clare, A. Rosenhahn, *Langmuir* **2021**, *37*, 5950.
[8] E. T. Iverson, H.-C. Chiang, T. J. Kolibaba, K. Schmieg, J. C. Grunlan, *Macromolecules* **2022**, *55*, 3151.
[9] S. Roy, N. M. Elbaz, W. J. Parak, N. Feliu, *ACS Appl. Bio Mater.* **2019**, *2*, 3245.
[10] M. Ishihara, S. Kishimoto, S. Nakamura, Y. Sato, H. Hattori, *Polymers* **2019**, *11*, 672.
[11] J. Luo, C. Shi, X. Qian, K. Zhou, *Mater. Chem. Phys.* **2022**, *291*, 126674.
[12] Q. Wang, J. B. Schlenoff, *Macromolecules* **2014**, *47*, 3108.
[13] K. Akkaoui, M. Yang, Z. A. Digby, J. B. Schlenoff, *Macromolecules* **2020**, *53*, 4234.
[14] S. Ali, V. Prabhu, *Gels* **2018**, *4*, 11.
[15] P. C. Suarez-Martinez, P. Batys, M. Sammalkorpi, J. L. Lutkenhaus, *Macromolecules* **2019**, *52*, 3066.
[16] T. Yuan, X. Cui, X. Liu, X. Qu, J. Sun, *Macromolecules* **2019**, *52*, 3141.
[17] A. Reisch, E. Roger, T. Phoeung, C. Antheaume, C. Orthlieb, F. Boulmedais, P. Lavalle, J. B. Schlenoff, B. Frisch, P. Schaaf, *Adv. Mater.* **2014**, *26*, 2547.
[18] H. Zhang, C. Wang, G. Zhu, N. S. Zacharia, *ACS Appl. Mater. Interfaces* **2016**, *8*, 26258.
[19] D. Meng, X. Liu, S. Wang, J. Sun, H. Li, Z. Wang, X. Gu, S. Zhang, *Compos. Part B Eng.* **2021**, *219*, 108886.
[20] S. T. Lazar, T. J. Kolibaba, J. C. Grunlan, *Nat. Rev. Mater.* **2020**, *5*, 259.
[21] J. J. Richardson, J. Cui, M. Björnmalm, J. A. Braunger, H. Ejima, F. Caruso, *Chem. Rev.* **2016**, *116*, 14828.
[22] M. A. Priolo, K. M. Holder, T. Guin, J. C. Grunlan, *Macromol. Rapid Commun.* **2015**, *36*, 866.
[23] Y. Zhang, P. Batys, J. T. O'Neal, F. Li, M. Sammalkorpi, J. L. Lutkenhaus, *ACS Cent. Sci.* **2018**, *4*, 638.
[24] S. Manoj Lalwani, C. I. Eneh, J. L. Lutkenhaus, *Phys. Chem. Chem. Phys.* **2020**, 10.1039.D0CP03696J.
[25] S. M. Lalwani, P. Batys, M. Sammalkorpi, J. L. Lutkenhaus, *Macromolecules* **2021**, *54*, 7765.
[26] R. F. Shamoun, A. Reisch, J. B. Schlenoff, *Adv. Funct. Mater.* **2012**, *22*, 1923.

[27] R. F. Shamoun, H. H. Hariri, R. A. Ghostine, J. B. Schlenoff, *Macromolecules* **2012**, *45*, 9759.
[28] J. Fu, H. M. Fares, J. B. Schlenoff, *Macromolecules* **2017**, *50*, 1066.
[29] T. J. Kolibaba, C.-C. Shih, S. Lazar, B. L. Tai, J. C. Grunlan, *ACS Mater. Lett.* **2020**, *2*, 15.
[30] G. A. Appuhamillage, N. Chartrain, V. Meenakshisundaram, K. D. Feller, C. B. Williams, T. E. Long, *Ind. Eng. Chem. Res.* **2019**, *55*, 15109.
[31] A. Bagheri, J. Jin, *ACS Appl. Polym. Mater.* **2019**, *1*, 593.
[32] N. H. Okoye, U. K. de Silva, J. A. Wengatz, Y. Lapitsky, *Polymer* **2015**, *60*, 69.
[33] U. K. de Silva, K. Choudhuri, A. C. Bryant-Friedrich, Y. Lapitsky, *Soft Matter* **2018**, *14*, 521.
[34] T. J. Kolibaba, N. A. Vest, J. C. Grunlan, *Mater. Chem. Front.* **2022**, 10.1039.D2QM00257D.
[35] E. M. Wilts, A. M. Pekkanen, B. T. White, V. Meenakshisundaram, D. C. Aduba, C. B. Williams, T. E. Long, *Polym. Chem.* **2019**, *10*, 1442.
[36] S. Khanlari, M. A. Dubé, *J. Macromol. Sci. Part A* **2015**, *52*, 587.
[37] J. Herzberger, V. Meenakshisundaram, C. B. Williams, T. E. Long, *ACS Macro Lett.* **2018**, *7*, 493.
[38] C. B. Arrington, M. Hegde, V. Meenakshisundaram, J. M. Dennis, C. B. Williams, T. E. Long, *ACS Appl. Mater. Interfaces* **2021**, *13*, 48061.
[39] F. Jiang, D. Drummer, *Polymers* **2020**, *12*, 1080.
[40] E. M. Wilts, A. Gula, C. Davis, N. Chartrain, C. B. Williams, T. E. Long, *Eur. Polym. J.* **2020**, *130*, 109693.
[41] C. Gorsche, K. Seidler, P. Knaack, P. Dorfinger, T. Koch, J. Stampfl, N. Moszner, R. Liska, *Polym. Chem.* **2016**, *7*, 2009.
[42] W. H. Carothers, *Trans. Faraday Soc.* **1936**, *32*, 39.
[43] L. De Keer, P. H. M. Van Steenberge, M.-F. Reyniers, D. R. D'hooge, *Polymers* **2021**, *13*, 2410.
[44] J. J. Schwartz, *MRS Bull.* **2022**, *47*, 628.
[45] D. E. Roberts, *J. Res. Natl. Bur. Stand.* **1950**, *44*, 221.
[46] J. Bennett, *Addit. Manuf.* **2017**, *18*, 203.
[47] Gelest, "Applying a Silane Coupling Agent," can be found under https://www.gelest.com/wp-content/uploads/09Apply.pdf, **n.d.**
[48] H. Gojzewski, Z. Guo, W. Grzelachowska, M. G. Ridwan, M. A. Hempenius, D. W. Grijpma, G. J. Vancso, *ACS Appl. Mater. Interfaces* **2020**, *12*, 8908.
[49] A. C. Uzcategui, C. I. Higgins, J. E. Hergert, A. E. Tomaschke, V. Crespo-Cuevas, V. L. Ferguson, S. J. Bryant, R. R. McLeod, J. P. Killgore, *Small Sci.* **2021**, *1*, 2000017.
[50] K. Choudhuri, J. D. Bastian, J. T. Berger, U. K. de Silva, Y. Lapitsky, *Colloid Polym. Sci.* **2022**, *300*, 707.
[51] H. H. Winter, F. Chambon, *J. Rheol.* **1986**, *30*, 367.
[52] L. E. Schmidt, Y. Leterrier, J.-M. Vesin, M. Wilhelm, J.-A. E. Månson, *Macromol. Mater. Eng.* **2005**, *290*, 1115.
[53] H. M. Fares, Q. Wang, M. Yang, J. B. Schlenoff, *Macromolecules* **2019**, *52*, 610.
[54] B.-S. Kim, S. W. Park, P. T. Hammond, *ACS Nano* **2008**, *2*, 386.
[55] J. J. Harris, P. M. DeRose, M. L. Bruening, *J. Am. Chem. Soc.* **1999**, *121*, 1978.
[56] W. Tomal, J. Ortyl, *Eur. Polym. J.* **2022**, *180*, 111588.
[57] Y. Zhang, Y. Li, V. K. Thakur, L. Wang, J. Gu, Z. Gao, B. Fan, Q. Wu, M. R. Kessler, *RSC Adv.* **2018**, *8*, 13780.
[58] Y. Bao, N. Paunović, J. Leroux, *Adv. Funct. Mater.* **2022**, *32*, 2109864.
[59] Q. Cui, D. J. Bell, S. B. Rauer, M. Wessling, *Adv. Mater. Interfaces* **2020**, 2000849.

[60] A. Andreu, P.-C. Su, J.-H. Kim, C. S. Ng, S. Kim, I. Kim, J. Lee, J. Noh, A. S. Subramanian, Y.-J. Yoon, *Addit. Manuf.* **2021**, *44*, 102024.
[61] F. Luo, T. L. Sun, T. Nakajima, T. Kurokawa, Y. Zhao, K. Sato, A. B. Ihsan, X. Li, H. Guo, J. P. Gong, *Adv. Mater.* **2015**, *27*, 2722.
[62] Y. Song, K. P. Meyers, J. Gerringer, R. K. Ramakrishnan, M. Humood, S. Qin, A. A. Polycarpou, S. Nazarenko, J. C. Grunlan, *Macromol. Rapid Commun.* **2017**, *38*, 1700064.
[63] P. J. Scott, V. Meenakshisundaram, M. Hegde, C. R. Kasprzak, C. R. Winkler, K. D. Feller, C. B. Williams, T. E. Long, *ACS Appl. Mater. Interfaces* **2020**, *12*, 10918.
[64] E. M. Maines, M. K. Porwal, C. J. Ellison, T. M. Reineke, *Green Chem.* **2021**, *23*, 6863.
[65] B. M. Stadler, J. G. de Vries, *Philos. Trans. R. Soc. Math. Phys. Eng. Sci.* **2021**, *379*, 20200341.

ToC

A polyelectrolyte complex is additively manufactured for the first time through vat photopolymerization. The mechanical properties of parts can be tuned through thermal treatment and by altering the resin chemistry. The ionic bonds which form these parts can be reversed through exposure to base and the part can be reprinted, showing promise for a circular 3D printing economy.

Thomas J. Kolibaba, Callie I. Higgins, Nathan C. Crawford, Joseph R. Samaniuk, and Jason P. Killgore**

Sustainable Additive Manufacturing of Polyelectrolyte Photopolymer Complexes

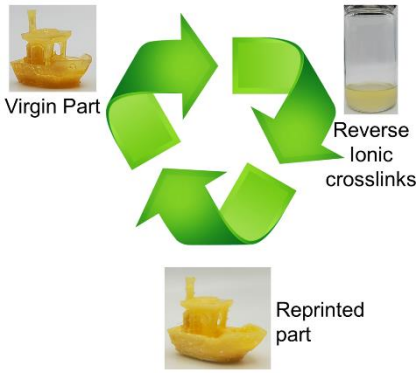

Supporting Information for

Sustainable Additive Manufacturing of Polyelectrolyte Photopolymer Complexes

Thomas J. Kolibaba, Callie I. Higgins, Nathan C. Crawford, Joseph R. Samaniuk, and Jason P. Killgore**

Example calculation for determine of MAA conversion via photoDSC:

Conversion in the photoDSC is measured by comparing measured reaction enthalpy in the DSC to the theoretical enthalpy of reaction according to the following equation:

$$\%Conversion = \frac{\Delta H_{rxn,measured}}{\Delta H_{theoretical}} * 100\ \% \quad (1)$$

The measured enthalpy of reaction, $\Delta H_{rxn,measured}$ is found in Table 1 and is 175 J g^{-1} for the 5 M resin. This must be normalized for the fraction of the resin that MAA accounts for (43 wt%) according to:

$$\Delta H_{rxn,measured} = 175 \frac{J}{g\ resin} * \frac{100\ g\ resin}{43\ g\ MAA} \approx 407\ \frac{J}{g\ MAA} \quad (2)$$

MAA has a molar mass of ca. 86 g mol^{-1}, the results from equation 2 can be multiplied by the molar mass to obtain a reaction enthalpy of 35 kJ mol^{-1}. The literature reaction enthalpy for methacrylic acid, $\Delta H_{theoretical}$, is 66 kJ mol^{-1}[45]. Use of these two values in equation 1 yields a %Conversion of ≈53 %.

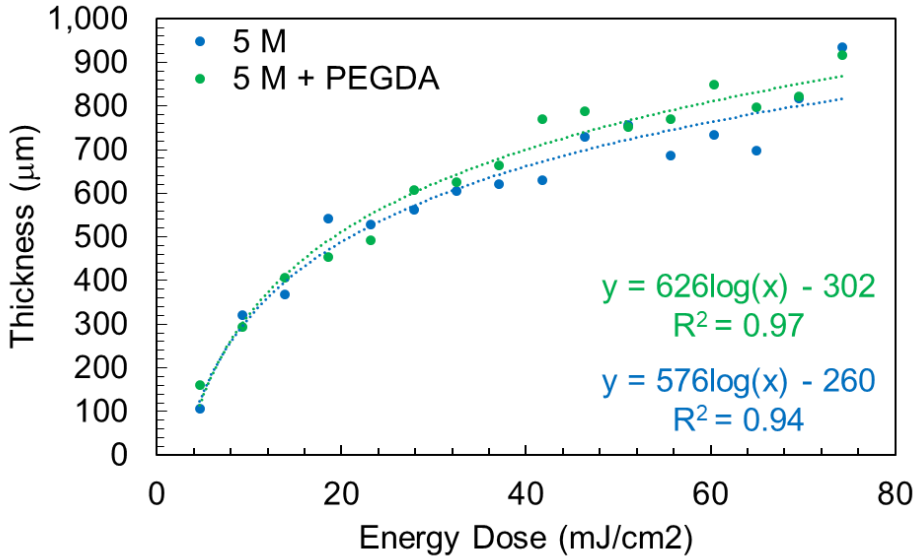

Figure S1. Working curve and corresponding fits for the 5 M Resin (blue) and the PEGDA Resin (green).

Table S1. Modulus values for the first 10 % (low-stress) and final 10 % (max-stress) of applied force in DMA compression testing.

Sample	*Low-Stress Modulus (kPa)*	*Max-Stress Modulus (kPa)*
5 M Dry	1,200 ± 300	11,000 ± 5000
5 M Wet	104 ± 9	780 ± 20
Cured 5 M Dry	3,900 ± 800	14,000 ± 1000
Cured 5 M Wet	240[a]	530[a]
PEGDA Dry	3,400 ± 400	32,000 ± 2000
PEGDA Wet	60 ± 10	630 ± 30
Cured PEGDA Dry	2,930 ± 10	30,000 ± 2000
Cured PEGDA Wet	210 ± 50	900 ± 200
Upcycled PEC	4,500 ± 1700	23,000 ± 6000
Upcycled PEC Wet	45 ± 3	1,500 ± 100

a) All but one sample under this condition failed during dimensional measurement and mechanical property data could not be acquired.

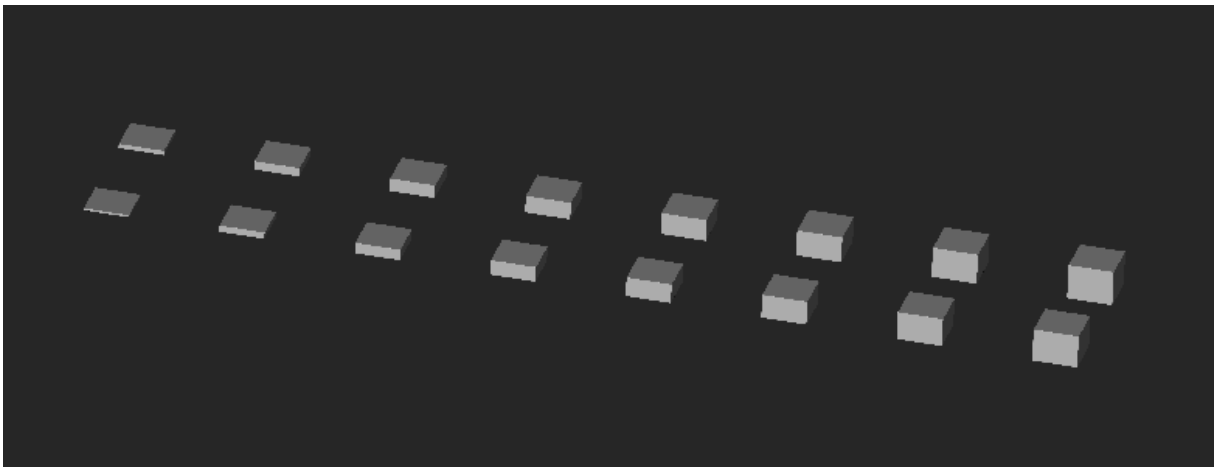

Figure S2. CAD model used for projection of the working curve. Each block measures 1x1 mm^2 at the base.